The development of an optimization procedure for the design of intelligent structures

Smart Mater. Struct. 2 (1993) 135–146. Printed in the UK

The development of an optimization procedure for the design of intelligent structures

Charles E Seeley and Aditi Chattopadhyay
Department of Mechanical and Aerospace Engineering, Arizona State University, Tempe, AZ 85281, USA

Received 19 April 1993, accepted for publication 7 June 1993

Abstract. Intelligent structures are structures which can actively react to an unpredictable environmental disturbance in a controlled manner. Piezoelectric materials are an excellent choice for the development of sensors and actuators for these structures due to their special properties. It is important to locate these discrete actuators optimally on the structure in order to achieve the most efficient implementation of their special properties. It is also necessary to design the structure to be controlled for optimum performance. This leads to a combined problem which includes the discrete actuator location problem and the continuous optimization problem involving control and structure interaction. A multiobjective optimization technique is used to formulate the problem. Optimum piezoelectric actuator thicknesses for the static case are determined for the active piezoelectric elements developed in this work. An optimization procedure is then presented which includes *actuator locations, vibration reduction, power consumption, minimization of* dissipated energy and maximization of the natural frequency as design objectives. The procedure is demonstrated through a cantilever beam problem. Results obtained indicate that improved structural and control performance can be obtained with only a few optimally placed actuators.

1. Introduction

An intelligent structure is characterized as a load bearing structure with the ability to actively sense and react to its environment via onboard sensors, actuators and computational/control capabilities. Many aerospace structures are constructed from light-weight composites and do not possess sufficient passive damping to reduce vibrations in order to avoid catastrophic results from an otherwise minor disturbance force. Conventional methods for controlling vibrations include the use of heavy stiffening members and/or non-structural tuning masses. An intelligent structure can sense the motion caused by a disturbance force and actively damp out unwanted vibrations to avoid problems at resonance with significantly less weight penalty.

Recently, there has been significant research interest in both the development and the application of various smart materials. A material that, when subjected to a mechanical load, accumulates an electric charge is said to have piezoelectric properties. Conversely, the piezoelectric material, when subjected to an applied electrical field, will induce strain. The polarity of the applied electrical field determines whether the strain is compressive or tensile. Due to the properties exhibited by piezoelectric materials, they are excellent candidates for active members of intelligent structures. Bailey and Hubbard (1985) used a distributed piezoelectric polymer, PVDF, for active vibration control of a cantilever beam. An analytical and experimental development of piezoelectric actuators as elements of intelligent structures resulted in a set of equations describing the effects of piezoelectric materials bonded to a substructure or embedded in a composite structure (Crawley and de Luis 1987). Anderson *et al* (1990) have discussed the development of an active element constructed of layered piezoceramic wafers. Optimal piezoelectric actuator thicknesses were discussed by Kim and Jones (1990) for surface bonded piezoelectric actuators. Heeg (1991) investigated the use of smart materials for the purpose of flutter suppression in both an experimental and an analytical setting including wind tunnel tests. Hanagud *et al* (1992) developed a finite elements model for a linearly elastic structure with bonded piezoelectric sensors and actuators. They also developed an optimal control procedure based on the minimization of a quadratic performance index.

It is desirable to distribute active structural members with built in sensing, feedback control and actuation functions optimally throughout an intelligent structure with a limited number of discretely placed actuators. Previously, for simple structures, researchers have relied

0964-1726/93/030135 + 12 $07.50

on trial and error techniques and engineering judgment for the best placement of active members (Heeg 1991, Hanagud *et al* 1985). Baily and Hubbard (1985) avoided this problem by assuming a continuous, rather than discrete, placement of the actuator across the top surface of a cantilever beam. These methods are not practical for larger and more complex structures. Recently, there has been some interest in using formal optimization strategies for the optimal placement of actuators throughout a structure. Onoda and Hanawa (1992) performed a comparison of the genetic algorithm (GA), worst out best in (WOBI), simulated annealing (SA) and the exhaustive single-point substitution (ESPS) approaches for the static shape control of a parabolic three-ring tetrahedral truss.

An alternative approach to the actuator placement problem involves continuous, rather than discrete, variables to describe the controlled structure. In this context, the problem is often approached from a control point of view. Schulz and Heimbold (1983) used dissipation energy as an objective with feedback gains as design variables to address the determination of optimal actuators with continuous variables. Horner and Walz (1985) used feedback gains to minimize the trace of the damping matrix as an objective function to determine optimal actuator locations, but noted that the optimal number of actuators was basically an engineering judgment.

Although these discrete and continuous methods are successful in determining optimal actuator locations, they do not address the influence of structural parameters that are continuous variables and that, when included as design variables, can enhance the performance of the distributed piezoelectric control system. For instance, a small change in the cross sectional area of the structural members can have a significant influence on the work required by the actuators to control the structure. Therefore when designing a structure for reduced vibration and the possible occurrence of resonance with a disturbance force while in service, it is equally important to determine the best locations for the discrete piezoelectric actuators on the structure. These are basically two distinct optimization problems to be solved: the first, a continuous structural problem, and the second, a discrete actuator location problem. The structural problem, which includes controls, is a conventional optimization problem that contains continuous design variables, such as cross sectional areas, from which derivatives can be calculated if a gradient based optimization procedure is used. The actuator location problem is an integer optimization problem for discretely placed sensors and actuators, which does not exhibit such derivatives. The combined problem of optimizing both the structure and the actuator locations leads to difficulties in the formulation of a gradient based optimization search. Likewise, integer optimization techniques do not lend themselves well to continuous optimization problems. Bailey and Hubbard (1985) pointed out the difficulty of using distributed parameter control theory with spatially discrete sensors and actuators. Koht *et al* (1986) investigated the use of cross sectional areas of structural members as design variables to minimize weight with constraints on the damping factors of the system. The net result was to enhance the active vibration control of a flexible structure by including structural parameters in the formulation. Miller and Shim (1987) investigated an optimization problem to reduce both the mass and the vibrational energy simultaneously. They pointed out the dependence of the optimal design on the initial conditions of the dynamic system. They also noted that if the desired result is mainly structural, such as mass minimization, the control system can be ignored in the optimization formulation, resulting in a much simpler problem. However, if control system performance is an issue, it must be included in the optimization problem. Another study by Koht and Veley (1990) investigated multiobjective optimization of the structure/control problem by minimizing structural mass and including additional objective functions as constraints such as natural frequencies and damping factors. More recently, Sepulveda *et al* (1992) investigated optimization involving structural/control synthesis where optimal locations of active members are treated as discrete variables which were made continuous over a series of explicit approximate problems using a branch and bound strategy.

The objective of the current research is the development of an optimization procedure to simultaneously address several different structural and control design criteria. Some initial investigation of the procedure has been presented by Chattopadhyay and Seeley (1993) in which the dissipated energy was minimized and the natural frequency was maximized simultaneously for a 2D truss. In the current research, optimal actuator thicknesses are determined for the static case by examining the optimal effective bending moment to stiffness ratio. Next, a cantilever beam example is presented to demonstrate the actuator location optimization algorithm through the systematic elimination of non-optimal actuator locations. Both structural and control design criteria are included in the formulation. Power requirements and vibration reduction are included as objective functions. The control design criteria include piezoelectric actuator placement, gains and actuator thicknesses. Structural design criteria include modifications of structural parameters for improved structural behavior. All of these design criteria are formulated simultaneously, rather than sequentially, using a multiobjective optimization technique (Chattopadhyay and McCarthy 1991). Such simultaneous treatment of the objective functions leads to significantly improved optimum results when compared to those obtained through a sequential treatment.

2. Model development

In order to better understand the mechanics of an intelligent structure, it is necessary to devise an accurate mathematical model. A finite element model of the

active box beam elements with piezoelectric actuators is developed. A state space control law is formulated using the relevant equations of motion. A procedure for evaluating system performance is also presented.

2.1. Active piezoelectric element

The simplest attachment of piezoelectric actuators to a metallic structure is surface bonding using a strong adhesive such as epoxy. It has been shown that for a thin bonding layer using a quality adhesive, the effects of the bonding layer on the efficiency of the actuators is negligible (Kim and Jones 1990). Therefore, surface bonded actuators with negligible bonding layer are used for this research. It is possible to embed sensors and actuators into a composite structure during manufacturing. This is not possible for metals due to the high temperatures involved during processing, which would destroy any piezoelectric material currently available. For simplicity, only metallic structural materials, such as aluminum and steel, are used in this study. It is also assumed that sensors and actuators are collocated in order to avoid problems with stability.

Figure 1 presents piezoelectric actuators that are attached in the same position on both the top and bottom surfaces of a flat plate. If the applied voltage to each actuator has the same polarity, as in figure 1(a), extension along the x axis will result since both actuators will act in the same direction. This is referred to as a unimorph configuration. Similarly, if the polarity is reversed for one of the actuators, as shown in figure 1(b), one will act in tension and the other in compression. This results in an effective bending moment applied to the plate at the location of the actuators and is known as a bimorph configuration.

Examining figure 1(a), in which both actuators act in the same direction, the strain distribution across the plate is constant and the strain in the piezoelectric actuators is also assumed to be constant. Figure 2 presents the forces which result from a piezoelectric material bonded to a substructure in the manner shown in figure 1(a). The force F resulting from this unimorph configuration is derived from a force balance between the actuators and the substructure (Crawley and de Luis 1987). Applying a force balance to the configuration shown in figure 2, the stresses in the substructure and the actuators are calculated as follows:

$$\sigma_B = \frac{2F}{bt_B} \tag{1}$$

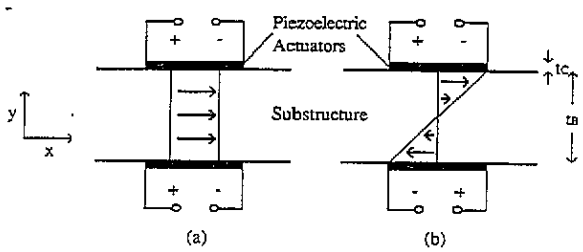

Figure 1. Strain distribution resulting from piezoelectric actuators: (a) some polarity top and bottom; (b) opposite polarity.

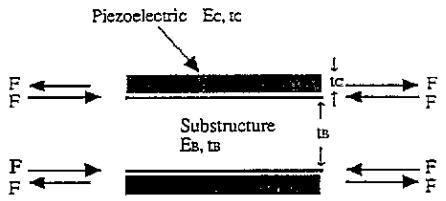

Figure 2. Force balance.

$$\sigma_C = -\frac{F}{bt_C} \tag{2}$$

where σ_B and σ_C are the stresses and t_B and t_C are the thicknesses of the substructure and the piezoelectric material, respectively. The quantity b represents the width of the beam and the actuators, which are assumed to be equal, and F is the resultant force. The stress–strain relationships reduce to the following:

$$\epsilon_B = \frac{\sigma_B}{E_B} \tag{3}$$

$$\epsilon_C = \frac{\sigma_C}{E_C} + \Lambda \tag{4}$$

where ϵ_B and ϵ_C are the strains and E_B and E_C are the elastic moduli of the substructure and the piezoelectrics, respectively. The quantity Λ is the strain resulting from the electromechanical coupling of the piezoelectric material and is defined as follows:

$$\Lambda = \frac{d_{31}V}{t_C} \tag{5}$$

where the parameter d_{31} is the piezoelectric strain constant and V is the applied voltage in the poling direction which is assumed to be the 3, or thickness, direction of the piezoelectric material. It must be noted that the strains in the substructure and the actuators are assumed to be constant. Therefore, from equations (1)–(4), an expression can be developed for the force resulting from the actuators:

$$F = \frac{E_B t_B b}{2 + \Psi}(-\Lambda). \tag{6}$$

The quantity Ψ is a dimensionless ratio relating the stiffness of the piezoelectric actuators to the stiffness of the substructure which is defined below:

$$\Psi = \frac{E_B t_B}{E_C t_C}. \tag{7}$$

Figure 3 shows a square box beam with uniform wall thickness t_B. If t_B and the thickness of the piezoelectric actuators t_C are significantly smaller than the height h of the beam, the strain distribution in the top and bottom webs of the box beam and the piezoelectric actuators is approximately constant for an applied bending moment, although opposite in sign. It is therefore desirable to have both of the top web actuators acting in the same direction. Similarly, it is desirable to have both the actuators on the lower web acting in a direction opposite to that of the actuators on the upper web. This results in an

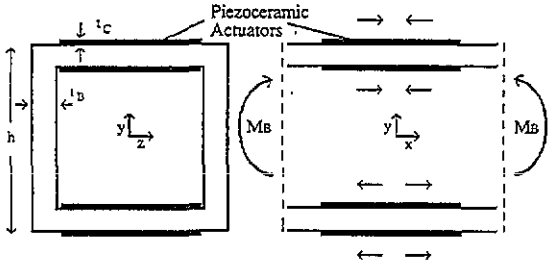

Figure 3. Placement of piezoelectric actuators on a box beam.

effective bending moment M given by

$$M = Fh. \tag{8}$$

2.2. Finite-elements model development

The finite-element method is used to model the structure and the active piezoelectric elements. The model begins with the common beam element formulation which includes transverse and rotational degrees of freedom. The axial degree of freedom is not important for this application and is therefore neglected. The stiffness properties of both the box beam and the actuators are included in the beam stiffness element formulation

$$\begin{bmatrix} \hat{f}_{1y} \\ \hat{m}_1 \\ \hat{f}_{2y} \\ \hat{m}_2 \end{bmatrix} = \frac{E_B I_B + E_C I_C}{L^3} \begin{bmatrix} 12 & 6L & -12 & 6L \\ 6L & 4L^2 & -6L & 2L^2 \\ -12 & -6L & 12 & -6L \\ 6L & 2L^2 & -6L & 4L^2 \end{bmatrix} \begin{bmatrix} \hat{d}_{1y} \\ \hat{\phi}_1 \\ \hat{d}_{2y} \\ \hat{\phi}_2 \end{bmatrix} \tag{9}$$

or

$$\hat{f} = \hat{\mathbf{k}}^* \hat{x} \tag{10}$$

where $\hat{f}$, $\hat{\mathbf{k}}^*$, and $\hat{x}$ are the force, the augmented element stiffness matrix and the displacement vector, respectively. The nodal displacements and rotations are denoted $\hat{d}$ and $\hat{\phi}$, respectively, and are elements of the vector $\hat{x}$ in the local coordinate system. The quantity I_B is the moment of inertia about the neutral axis of the beam and L is the element length. The moment of inertia I_C of the actuators, is calculated by integrating through the thickness of the actuators with respect to the neutral axis of the beam. It is zero for elements which do not contain piezoelectric actuators. The symbol * is used to indicate that the beam element stiffness matrix has been augmented with the stiffness properties of the piezoelectric actuators. The beam element consistent mass matrix is constructed in a similar fashion and is expressed as follows:

$$\begin{bmatrix} \hat{f}_{1y} \\ \hat{m}_1 \\ \hat{f}_{2y} \\ \hat{m}_2 \end{bmatrix} = \frac{\rho_B A_B L + \rho_C A_C L}{420} \times \begin{bmatrix} 156 & 22L & 54 & -13L \\ 22L & 4L^2 & 13L & -3L^2 \\ 54 & 13L & 156 & -22L \\ -13L & -3L^2 & -22L & 4L^2 \end{bmatrix} \begin{bmatrix} \ddot{\hat{d}}_{1y} \\ \ddot{\hat{\phi}}_1 \\ \ddot{\hat{d}}_{2y} \\ \ddot{\hat{\phi}}_2 \end{bmatrix} \tag{11}$$

or

$$\hat{f} = \hat{\mathbf{m}}^* \ddot{\hat{x}} \tag{12}$$

where ρ_B is the density of the beam material, A_B is the beam element cross sectional area and the double dots indicate a second derivative with respect to time. It must be noted that the piezoelectric actuator density ρ_C and the cross sectional area A_C are non-zero only at actuator locations on the structure. Transformation to the global set of coordinates is obtained by pre- and post-multiplying the element mass and stiffness matrices by a suitable coordinate transformation matrix $\mathbf{T}$:

$$\mathbf{k}^* = \mathbf{T}^T \hat{\mathbf{k}}^* \mathbf{T} \tag{13}$$

$$\mathbf{m}^* = \mathbf{T}^T \hat{\mathbf{m}}^* \mathbf{T} \tag{14}$$

where $\mathbf{k}^*$ and $\mathbf{m}^*$ are the augmented element stiffness and mass matrices of the substructure in global coordinates, respectively. It is important to note that this is a two-dimensional formulation, therefore the moment about the z axis is the same in both local and global coordinates. The augmented element stiffness and mass matrices in global coordinates are then used to derive the augmented global matrices $\mathbf{K}^*$ and $\mathbf{M}^*$ using a standard technique (Bickford 1990) where the properties of the piezoelectric actuators are only included at locations where the active elements exist.

Using equation (6), the moment resulting from the piezoelectric actuators bonded to a square box beam is expressed as

$$M = \frac{E_B t_B b h}{2 + \Psi}(-\Lambda). \tag{15}$$

The voltage V_i applied to the ith discrete piezoelectric actuator is represented as follows:

$$V_i = G_i \dot{\phi}_i \tag{16}$$

where G_i is the gain and $\dot{\phi}_i$ is the angular velocity of the beam at the location of the ith piezoelectric actuator. In the above equation, the single dot indicates a derivative with respect to time. Assuming a square cross section, the bending moment M on the box beam can be expressed as follows:

$$M = \frac{E_B t_B h^2}{2 + \Psi}\left(\frac{d_{31} G_i \dot{\phi}_i}{t_C}\right). \tag{17}$$

A gain matrix is formulated to model the active properties of the piezoelectric actuators. The in plane force exerted by each actuator, which is the major force exerted by the actuator on the structure, does not contribute directly to any other structural response other than creating a bending moment at the location of the discrete actuator (Chaudhry and Rogers 1992). This is equivalent to applying a suitable moment to the nodes of each active piezoelectric element (Hanagud *et al* 1992). The actuators are designed to create a moment about the z axis of each active element proportional to the rotational velocity of the element, which requires including a velocity gain in the matrix of each active

element:

$$\begin{bmatrix} \hat{f}_{1y} \\ \hat{m}_1 \\ \hat{f}_{2y} \\ \hat{m}_2 \end{bmatrix} = \frac{E_B t_B h^2}{2+\Psi} \frac{d_{31}}{t_C} \begin{bmatrix} 0 & 0 & 0 & 0 \\ 0 & G_i & 0 & -G_i \\ 0 & 0 & 0 & 0 \\ 0 & -G_i & 0 & G_i \end{bmatrix} \begin{bmatrix} \hat{d}_{1y} \\ \hat{\phi}_1 \\ \hat{d}_{2y} \\ \hat{\phi}_2 \end{bmatrix} \quad (18)$$

or

$$\hat{f} = \hat{\mathbf{c}}\hat{\dot{x}} \quad (19)$$

where $\hat{\mathbf{c}}$ is the element active damping matrix. Since the gain matrix only corresponds to the rotational degrees of freedom, its value is the same in both local and global coordinates and does not require the use of the transformation matrix **T**. The effect of the gain matrix is equivalent to conventional viscous damping, although the damping force is due to the active controls rather than a passive effect. The global gain matrix is denoted **C**.

2.3. Equations of motion and control law

The global second-order equation of motion without damping and forcing function is written as

$$\mathbf{M}^*\ddot{x} + \mathbf{K}^* x = \mathbf{0} \quad (20)$$

where $x = [y_1, \phi_1, y_2, \phi_2, \ldots]^T$. A disturbance force F is applied to the uncontrolled structure over a time interval $0 \leqslant t \leqslant t_a$, which leads to the following equation of motion:

$$\mathbf{M}^*\ddot{x} + \mathbf{K}^* x = F. \quad (21)$$

The actuators become active during a time period $t_a \leqslant t \leqslant t_b$ in order to damp out the vibrations caused by the disturbance during the previous time period. The $2n$ state space control law is written as

$$\frac{d}{dt}\begin{bmatrix} x \\ \dot{x} \end{bmatrix} = \mathbf{A}\begin{bmatrix} x \\ \dot{x} \end{bmatrix} + \mathbf{B}[u] \quad (22)$$

where

$$\mathbf{A} = \begin{bmatrix} \mathbf{0} & \mathbf{I} \\ -\mathbf{M}^{*-1}\mathbf{K}^* & \mathbf{0} \end{bmatrix} \quad (23)$$

$$\mathbf{B} = \begin{bmatrix} \mathbf{0} \\ -\mathbf{M}^{*-1}\mathbf{C} \end{bmatrix}. \quad (24)$$

In the above equations, **I** is the identity matrix and **C** is the gain matrix. Negative velocity feedback (rate feedback) is used in conjunction with the gain matrix. Since $[u] = [\dot{x}]$, the control gain matrix acts in the same way as a structural damping matrix. Therefore, the actuators assume the role of active damper elements. Any passive structural damping is considered negligible. Finally, the undamped system is checked during the time interval $t_b \leqslant t \leqslant t_c$ to ensure that the total energy of the system and the displacements have been reduced to a specified value.

$$\mathbf{M}^*\ddot{x} + \mathbf{K}^* x = \mathbf{0}. \quad (25)$$

The equations of motion and the state space control law are transformed into modal space by using modal summation techniques. This transformation has considerable computational advantages and also eliminates problems related to controlling higher modes which do not have significant contributions to the overall motion. Four modes are retained in this study. The active damping matrix **C** is not proportional to the mass and stiffness matrices, so techniques which take advantage of that situation are not applicable here. As a result, the equations do not decouple.

3. Optimization formulation

In this section, a description of the optimal actuator location algorithm is provided. This is followed by details of the coupled structure/control optimization problem formulation. Objective functions, constraints, and design variables are discussed.

3.1. Actuator location optimization

An optimization procedure is developed in which the choice of optimal actuator locations is made on the basis of the energy dissipated by the actuator at each location (Chattopadhyay and Seeley 1993). Actuator locations which have small contributions to the overall reduction of the energy in the system are eliminated. Only actuator locations with significant contributions to the dissipated energy are retained. Actuators are initially located on each structural element. Next, the total dissipated energy is minimized and the energy dissipated by each actuator is determined. Actuator locations with significantly less energy dissipation compared to the remaining actuators are eliminated as possible locations, a few at a time, by setting their gains to zero. This involves restarting the optimization procedure several times once convergence is obtained for each actuator configuration. The optimal configuration is reached when the removal of additional actuators leads to violation of one or more of the constraints, or an increase in the objective function value is observed.

3.2. Objective functions

The optimum design of intelligent structures is associated with several design criteria. The criteria included as objective functions in this paper are detailed in this section. One of the objectives is to determine the optimal locations of the actuators by minimizing the energy dissipated by them. The energy dissipated by each actuator can be expressed as the integral over the time period of active control ($t_a \leqslant t \leqslant t_b$) for each actuator. The total energy J to be minimized is the sum of these integrals and is given as follows:

$$J = \sum_{i=1}^{I_{ACT}} \int_{t_a}^{t_b} \dot{x}_i^T \mathbf{c}_i \dot{x}_i \, dt \quad (26)$$

where I_{ACT} is the current number of elements which are considered as possible actuator locations and $\mathbf{c}_i$ is the

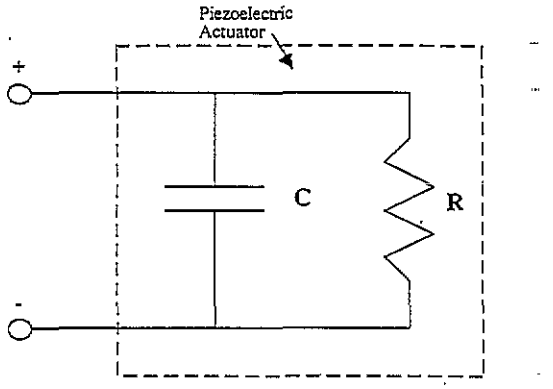

Figure 4. Piezoelectric actuator represented as a parallel *RC* circuit.

individual gain matrix of the ith active damping element. The total energy J can also be viewed as a quadratic performance index from a control standpoint using the gain matrix as the arbitrary weight matrix which has real physical significance in this case.

Power requirements for a piezoelectric control system are an important issue in critical aerospace applications (Rogers 1993). It is desirable to minimize the amount of electrical energy U required by the actuators to control the structure. Therefore, it is used as an objective function. Piezoelectric actuators can be modelled as an *RC* circuit in parallel, as shown in figure 4, where R_i is the resistivity and C_i is the capacitance of the ith piezoelectric actuator. The electrical energy U is an integral of power over time and is summed over all of the actuators for the total electrical energy which is expressed as follows:

$$U = \sum_{i=1}^{I_{ACT}} \int_{t_a}^{t_b} \left\{ \frac{V_i^2}{R_i} + C_i V_i \frac{dV_i}{dt} \right\} dt. \tag{27}$$

In the above equation, V_i is the voltage of the ith actuator.

Vibration reduction is an important design criterion. Minimization of a performance index defined by the integral absolute error (IAE) criterion (Ogata 1990) is suitable for reducing overall vibrational amplitudes and is expressed as follows:

$$\int_{t_a}^{t_b} |e(t)|\, dt \tag{28}$$

where $e(t)$ is the error in the system. Minimization of the IAE criterion results in a system with reasonable damping and a satisfactory transient response characteristic. It is also easily evaluated numerically. Therefore, the IAE criterion is used as an objective function which is minimized during optimization to reduce oscillatory motion. Since the desired input of the system approaches zero, the error can be represented simply as the state vector:

$$e(t) = \begin{bmatrix} x \\ \dot{x} \end{bmatrix} \tag{29}$$

where x is the vector of displacements and velocities. The integral is evaluated numerically over each component of the state vector and a 2-norm of the resultant vector is used to facilitate its usefulness in the optimization procedure. Finally, the fundamental frequency ω_1 is maximized to avoid possible resonance with the forcing frequency and thereby help reduce vibration.

3.3. Constraints

The design criteria that are formulated as constraints are discussed in this section. It is desired that the total energy E of the structure, which is the sum of the potential and the kinetic energies, is reduced to a specified fraction of the original energy after the time interval $T = t_b - t_a$. Therefore, a constraint is imposed as follows:

$$E_{fin} \leqslant \gamma E_{int} \tag{30}$$

where E is the energy and the subscripts 'int' and 'fin' refer to the initial and the final states, respectively. The quantity γ is the desired fraction of the initial energy remaining in the system after the specified time T.

A piezoelectric material is associated with a maximum electric field E_{max}. Exceeding this value can result in the loss of the material's special properties. Corresponding, there exists a maximum voltage V_{max} that can be applied to a piezoelectric actuator and that must not be exceeded. The voltage is checked at each time step of the numerical equation solver. Noting that $V_i = G_i \dot{\phi}_i$ for each actuator (equation (16)), when $V_i \geqslant V_{max}$, saturation occurs and the gain for the next time step for that actuator is set to

$$G_i = \frac{V_{max}}{\dot{\phi}_i}. \tag{31}$$

This ensures that $V_i \leqslant V_{max}$ without introducing any new design variables. As the rotational velocity increases, the voltage to each actuator remains constant and does not exceed the maximum allowable voltage. As the number of actuators is reduced during the optimization process, the voltage to the remaining actuators increases in order to redistribute the control forces necessary for satisfying all of the constraints. As a result, this constraint becomes more active.

The desired modal damping ratio $\bar{\zeta}_j$, corresponding to the jth mode, can be expressed as

$$\bar{\zeta}_j = \frac{\ln(1/\kappa)}{\omega_j T} \tag{32}$$

where ω_j is the jth undamped natural frequency of the structure and κ is the fraction of the initial vibration amplitude which remains after the time interval T. Upon calculation of ζ_j, the actual damping ratio corresponding to the jth mode, the following constraint is imposed to ensure that the desired damping ratios are achieved:

$$\zeta_j \geqslant \bar{\zeta}_j. \tag{33}$$

The gain matrix $\mathbf{C}$ is not constant since it must be altered at each time step to ensure that the voltage does not exceed V_{max}. Therefore, ζ_j is not constant over time either. A minimum gain matrix is obtained at maximum velocity when saturation occurs. The maximum gain matrix is found when V_{max} is not exceeded by any one

of the actuators. To evaluate the damping ratio constraint, constant damping ratios are determined by using a gain matrix which is averaged over the time interval when the actuators are active. Although these averaged damping ratios cannot be used to construct an analytical solution of the decaying motion, they approximately describe the character of the solution to ensure that proper damping does occur in the desired modes. The weighted average will fit between the minimum and the maximum damping factors calculated from the minimum and the maximum gains, respectively.

Since the mass can increase in an effort to stiffen the structure and thereby minimize the energy dissipated by the actuators, a constraint is also imposed on the total mass m of the structure:

$$m \leqslant \bar{m} \tag{34}$$

where $\bar{m}$ is the allowable value.

3.4. Design variables

A single gain, representing all actuators, is used as a design variable. Other design variables include the cross sectional areas of each box beam element. The piezoelectric actuator thicknesses are also included as design variables.

4. Optimization implementation

The optimizer used in this study consists of a non-linear programming procedure for constrained function minimization based on the method of feasible directions, as implemented in the computer code CONMIN (Vanderplaats 1973). The optimization process is initiated by defining all the necessary parameters for the initial design. Next, a function analysis is performed to calculate objective function and constraint information. This is followed by a sensitivity analysis for determining gradients of both the objective function and the constraints using a forward finite-difference technique. The optimization procedure is continued until convergence is obtained. Convergence is based on three consecutive values of the objective function changing by less than 0.5%.

Since CONMIN requires several evaluations of the objective function and constraints during its search for a feasible design point, the use of an exact analysis for each calculation can be computationally prohibitive. Therefore, an approximation technique known as the two-point exponential approximation (a hybrid technique) developed by Fadel *et al* (1990), is used. The two-point exponential approximation is an extension of a Taylor series approximation that employs an exponential function that uses design variables and gradient information from the previous and current design points. To reduce possible errors while using either of the above approximation schemes, move limits, defined as the maximum fractional change of a design variable value, are imposed as upper and lower bounds on the design variables. Further details of this procedure are presented by Chattopadhyay and Seeley (1993).

The optimization of an intelligent structure involves the design of the structure as well as the control system and the actuator locations. Each discipline represents different design objectives which are to be optimized. However, conventional optimization techniques are posed as the minimization of a single objective function subject to a certain number of constraints. To efficiently formulate an optimization problem which involves multiple design objectives, a multiobjective formulation technique known as the minimum-sum beta (Min $\Sigma\beta$) approach (Chattopadhyay and McCarthy 1991) is used. A single composite objective function is developed which represents the best possible compromise between the original objective functions as it is minimized during the optimization procedure. The objective function is linear and provides computational advantages. The procedure also avoids the necessity of using arbitrary weight factors which are often used in solving multiobjective problems.

5. Optimization of actuator thicknesses

The concept of an optimal piezoelectric actuator thickness for the static case can be addressed by examining equation (15):

$$M = \frac{E_B t_B b h}{2 + \Psi}(-\Lambda).$$

In the above equation, the bending moment M from the piezoelectric actuators approaches zero when the actuator stiffness approaches zero, which causes Ψ to become large. This indicates that an infinitely thin actuator will have virtually no effect in producing a bending moment. The moment again approaches zero when the piezoelectric actuator thickness, and thus the stiffness, becomes infinitely large. This is because the flexural rigidity of the actuator limits the allowable bending strain. Consequently, the interface stress between the actuator and beam becomes small, thus reducing the bending moment. Therefore, there must exist a non-zero value of the actuator thickness, between the limiting cases, which produces a maximum effective moment.

Consider a box beam with bonded piezoelectric actuators on the upper and lower surfaces of both the top and bottom webs, which is the configuration used for the current study (figure 3). The standard moment–curvature relation for this configuration is expressed as

$$M = (E_B I_B + E_C I_C)\frac{\mathrm{d}v^2}{\mathrm{d}x^2} \tag{35}$$

where M is the bending moment, the quantities $E_B I_B$ and $E_C I_C$ represent the beam and actuator stiffnesses, respectively, and v is the transverse displacement. The maximum effective bending moment induced by the actuators occurs when the bending moment M is a maximum compared to the stiffness of the beam and the piezoelectric actuators. This optimum value is

associated with the maximum value of the ratio

$$\Omega = \frac{M}{(E_B I_B + E_C I_C)}. \tag{36}$$

It must be noted that the ratio Ω is a function of the effective bending moment M, the stiffnesses of both the beam and the actuators, the applied voltage and the dimensions of both the actuators and the substructure.

From equation (5), it is also seen that the piezoelectric strain Λ is proportional to the applied electric field V/t_C and the proportionality constant d_{31} which is the piezoelectric strain constant and represents the degree of electromechanical coupling of the peizoelectric material. Since the effective moment is directly proportional to the piezoelectric strain constant d_{31} (equation (17)), to maximize the effective bending moment, a material with a high piezoelectric strain constant is desirable. However, the value of the piezoelectric strain constant merely acts as a multiplying factor in the evaluation of the piezoelectric strain (equation (5)) and is independent of the optimal thickness t_C of the piezoelectric actuators.

From equation (17), it appears that theoretically much greater moments can be expected with thinner piezoelectric actuators under a constant applied voltage. However, this observation is impractical because piezoelectric materials are associated with a maximum allowable electric field strength. If the maximum allowable electric field strength is exceeded, the material loses its special piezoelectric properties. Thus, in order to accurately optimize actuator thicknesses in a meaningful manner, the electric field strength must be held constant, instead of the applied voltage, to correctly represent the physical nature of piezoelectric materials.

It is also important to note that the deflection varies with the height h of the beam. An increase in h increases the moment arm of the actuators, thereby increasing the applied bending moment independent of the actuator thickness. Therefore, h must be held constant for a meaningful optimization of actuator thicknesses.

The maximum effective moment also depends on the properties of the beam and the piezoelectric actuator materials. Although these material properties will have an impact on the optimal actuator thicknesses, they are typically predetermined and are therefore not varied during optimization. Aluminum and steel are the readily available structural materials which are considered for this study. PZT G-1195 piezoceramics are used for the actuators.

It is desirable to create a non-dimensional actuator thickness t^* where $t^* = t_C/t_B$. Using equations (17) and (36), the ratio Ω is expressed, in terms of the non-dimensional thickness, as follows:

$$\Omega = \frac{E_B t_B h^2 d_{31} E_{max}}{(2 + E_B/E_C t^*)(E_B I_B + E_C I_C)} \tag{37}$$

where E_{max} is the maximum allowable electric field. It must be noted that the moments of inertia I_B and I_C are also functions of t^*. Holding E_B, E_C, L and h fixed with the material constants d_{31} and E_{max} set to their respective values, it is now meaningful to examine the variation of the ratio Ω as a function of t^*. The optimal value of t^*, corresponding to the largest value of the ratio Ω, results in the maximum effective moment and is presented in figure 5. From figure 5, it is observed that the ratio Ω approaches zero in the limiting cases of actuator thicknesses approaching either zero or infinity, as expected.

The optimal thickness corresponding to the maximum value of Ω, and thus the maximum effective moment for an aluminum box beam with PZT actuators, is found to be 0.61 over a range of box beam web thicknesses (0.5–50.0 mm) and heights (50–500 mm). The corresponding value for steel is 1.91. The optimal value of t^* is higher for steel because the piezoelectric material is relatively less stiff than for aluminum. It must be noted that these values differ from a previous study (Kim and Jones 1990) which used PZT G-1195 actuators for both an aluminum and a steel plate. This is because a bimorph configuration of actuators was used in that study, whereas a unimorph configuration is used in the current study. In general, the same trends are observed. For example, stiffer actuators compared to the substructure are desirable to increase actuator effectiveness. Therefore, piezoceramic materials are more desirable as actuators than PVDF due to their higher elastic moduli. PZT is the piezoceramic material which is implemented in the actuators used in this study because of its high-stress and low-strain characteristics when compared to polymer piezoelectrics such as PVDF, which are better suited for sensing, as opposed to actuation, applications. It is also important to realize that these optimal values correspond to the static bending case only, although many of the same trends can be observed in the dynamic case as well.

6. Actuator placement for a coupled control–structure problem

Four objective functions are included in this study in addition to the optimal actuator location problem for a cantilever box beam. The energy J dissipated by the actuators is minimized to facilitate the actuator location algorithm. Vibration is reduced by minimizing the IAE

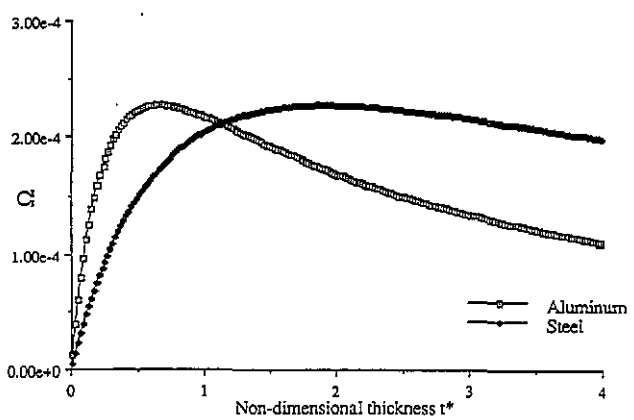

Figure 5. Non-dimensional actuator thickness.

Table 1. Piezoelectric and material properties (Kvnar 1987).

Property	Variable	Value	Units
PZT G-1195			
Piezoelectric strain constant	d_{31}	166×10^{-12}	$m V^{-1}$
Density	ρ_C	7600	$kg m^{-3}$
Elastic modulus	E_C	63×10^9	$N m^{-2}$
Maximum electric field	E_{max}	600×10^3	V
Aluminum			
Density	ρ_B	2800	$kg m^{-3}$
Elastic modulus	E_B	68.5×10^9	$N m^{-2}$
Steel			
Density	ρ_B	7750	$kg m^{-3}$
Elastic modulus	E_B	200×10^9	$N m^{-2}$

criterion. Power requirements of the actuators are minimized by including the total electrical energy consumption U as an objective function. Finally, the natural frequency ω_1 of the structure is maximized to reduce the possibility of resonance with the forcing function.

Constraints are imposed on the displacement amplitudes in the form of lower bounds on the damping ratios. The vibrational amplitudes, corresponding to the first four modes, must be reduced to 5% of their original values within 1s from the action of the control system. Any passive damping is neglected. The total energy in the system, which is the sum of the kinetic and potential energies, is also reduced to 5% of its original value within 1s. The voltage applied to the piezoelectric actuators is not permitted to exceed the maximum electric field E_{max} as recommended by the manufacturer of the PZT actuators. The optimization is performed with aluminum and steel beam materials. PZT G-1195 piezoceramics are used for actuators in both cases. Material properties of the aluminum, steel and piezoceramic actuators used in this study are presented in table 1. The disturbance is caused by a sinusoidal force of magnitude 220 N, at a frequency of 25 Hz, applied at the tip of the beam for 0.067 s. The constraints are identical for both cases except for the mass constraint ($m \leqslant \bar{m}$). A value of $\bar{m} = 10$ kg is used for aluminum and a value of $\bar{m} = 22$ kg is used for steel. Lower and upper bounds are also placed on the design variable values. Actuator thicknesses t_{C_i} are constrained to be approximately in the range of currently available PZT

Table 2. Actuator configuration iteration history: aluminum.

Iteration	Elements which contain actuators
Initial	10, 9, 8, 7, 6, 5, 4, 3, 2, 1
A	10, 9, 8, 7, 6, 5, 4, 3, 2, 1
B	9, 8, 7, 6, 5, 4, 3, 2, 1
C	8, 7, 6, 5, 4, 3, 2, 1
D	7, 6, 5, 4, 3, 2, 1
E	6, 5, 4, 3, 2, 1
F	5, 4, 3, 2, 1
G	4, 3, 2, 1
H	3, 2, 1
I	2, 1

Table 3. Design variable iteration history: aluminum.

Iteration	Gain ($\times 10^{-3}$ V s m^{-1})	Actuator thickness (mm)	Cross-sectional area ($\times 10^{-3}$ m^2)
Initial	1.00	0.30	1.20
A	0.96	0.31	1.34
B	0.96	0.31	1.37
C	0.95	0.32	1.40
D	0.95	0.30	1.46
E	0.97	0.40	1.42
F	1.06	0.40	1.47
G	1.12	0.40	1.53
H	1.49	0.40	1.58
I	2.33	0.40	1.65

G-1195 piezoelectric sheets ($0.1\,\text{mm} \leqslant t_{C_i} \leqslant 0.4\,\text{mm}$). To ensure stability, actuator gains G_i are constrained to be positive ($G_i \geqslant 0$). The gains of all of the current actuators are assumed to be equal and are represented through a single design variable. This considerably reduces the computational effort during optimization. Each of the cross sectional areas in the finite-element discretization of the cantilever box beam and the corresponding actuator thicknesses are also assumed to be equal. The web thickness of the box beam is assumed to be proportional to the cross sectional area. Sectional properties such as I, h and t_B are then computed from each area. Therefore a total of three design variables is used to represent actuator gain, cross sectional areas and actuator thicknesses. In the initial design for both cases (aluminum and steel), actuators with thickness 0.3 mm are located at each structural element of cross sectional area $A = 1.2 \times 10^{-3}$ m^2 and the displacement constraints are violated.

Optimization results for the aluminum beam are presented in tables 1–3 and figures 6–9. The optimization procedure is initiated by optimizing the initial design until the convergence criterion is satisfied. This point is defined as iteration A in table 2, which presents the actuator configuration iteration history. It must be noted that each iteration represents a fully converged design for that particular actuator configuration. The actuator at element 10 dissipates significantly less energy than the remaining actuators. Therefore, in accordance with the actuator location algorithm, it is eliminated from the set of possible actuator locations. The new configuration is then optimized. Upon convergence, it is labeled as iteration B. The actuator at element 9 is removed next and the process is systematically repeated

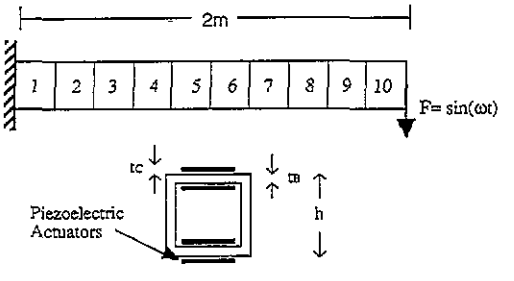

Figure 6. Ten-element cantilever beam and cross section.

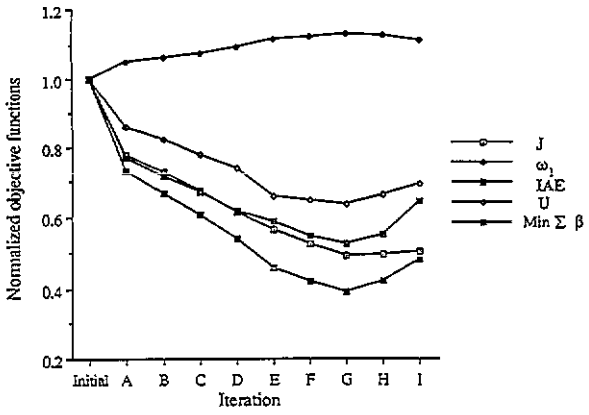

Figure 7. Normalized objective functions: aluminum.

until actuators are located only at elements 1 and 2. The four individual objective functions and the composite Min $\Sigma\beta$ objective function, each normalized with respect to their initial values at each iteration, are presented in figure 7. It is observed that there is a significant reduction in the objective function values from respective initial design values to iteration A, except for ω_1, which increases because it is maximized during the optimization procedure. This trend continues from iteration A to iteration G which corresponds to a reduced number of actuators. From iteration G to iteration I, all of the objective functions increase, except for ω_1, which decreases. Although the beam can be controlled with only two actuators (iteration I), the best design corresponds to iteration G using four actuators. Here, the dissipated energy J, the index IAE and the total electrical energy U are all at a minimum and ω_1 is at a maximum compared to the other iterations. It is clear that the smallest number of actuators is not necessarily the best number of actuators for vibration control. The voltage constraint becomes active during the first part of the control period as shown in figure 8. Without this constraint, large spikes may occur in the voltage which could damage the piezoelectric actuators. Figure 9 presents the variation of tip displacement with time, indicating that the displacement constraints are indeed satisfied. The design variable iteration history is presented in table 3. The optimum value of the dimensionless actuator thickness t^* for the static case of PZT actuators bonded to an aluminum box beam has been found to be 0.61. However, since dynamic effects were

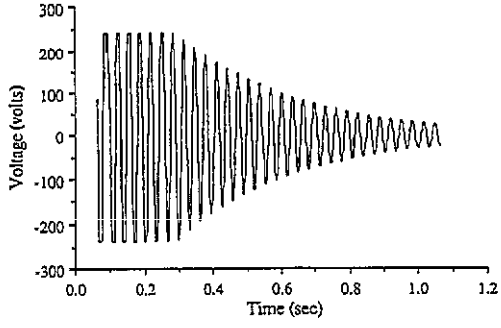

Figure 8. Voltage applied to actuator 1, iteration G: aluminum.

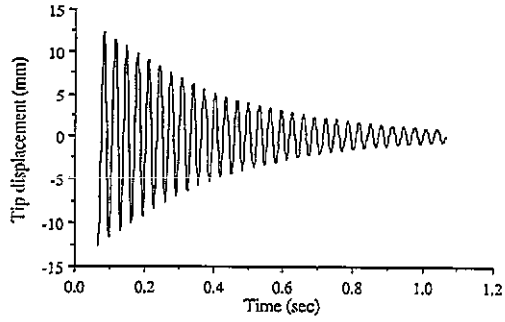

Figure 9. Tip displacement, iteration G: aluminum.

not included in the determination of this value, the actuator thicknesses are included as design variables to determine the dynamic effects. As with the static case, there are competing forces between actuator effectiveness, which tends to decrease thickness and stiffness, and maximum electric field E_{max}, which tends to increase the optimal thickness. Additionally, inertial effects of the actuator masses tend to reduce the optimal thickness, since lighter actuators are more efficient. The initial actuator thicknesses are set to 0.3 mm. Although a greater effective moment is generated by thicker actuators, inertial effects due to the mass of the actuators that reduce ω_1 prevent the thickness from increasing significantly during the first several iterations. At iteration E, inertial effects are no longer as important with the reduced set of actuators, and stiffness dominates. Therefore, the actuator thicknesses are driven to the upper bound of 0.4 mm and remain constant for subsequent iterations. The mass of the beam increases as actuators are removed from the beam in order to stiffen the structure with the remaining actuators while satisfying the mass constraint. The best cross sectional area, which is directly related to the mass, is found at iteration G. The gain must increase because the remaining actuators must do more work to control the beam as possible actuator locations are eliminated.

The optimum results for the steel box beam are presented in tables 4 and 5 and figures 10–12. Similar trends are observed for the steel box beam, although important distinctions must be pointed out. The initial design for the steel beam also violates the displacement constraint of the first mode. The actuator location iterations for steel are similar to the aluminum case, where actuator locations are first eliminated at the tip

Table 4. Actuator configuration iteration history: steel.

Iteration	Elements which contain actuators
Initial	10, 9, 8, 7, 6, 5, 4, 3, 2, 1
A	10, 9, 8, 7, 6, 5, 4, 3, 2, 1
B	9, 8, 7, 6, 5, 4, 3, 2, 1
C	8, 7, 6, 5, 4, 3, 2, 1
D	7, 6, 5, 4, 3, 2, 1
E	6, 5, 4, 3, 2, 1
F	5, 4, 3, 2, 1
G	4, 3, 2, 1
H	3, 2, 1
I	2, 1

Table 5. Design variable iteration history: steel.

Iteration	Gain ($\times 10^{-3}$ V s m^{-1})	Actuator thickness (mm)	Cross-sectional area ($\times 10^{-3}$ m^2)
Initial	2.25	0.30	1.20
A	2.32	0.40	1.21
B	2.34	0.40	1.23
C	2.36	0.40	1.25
D	2.36	0.40	1.27
E	2.40	0.40	1.29
F	2.53	0.40	1.31
G	2.77	0.40	1.33
H	3.35	0.40	1.35
I	5.47	0.40	1.36

and proceed towards the root as shown in table 4. Figure 10 presents the normalized objective functions. Again, each point represents a fully converged design. It is interesting to note that although the Min $\Sigma\beta$ objective function and the IAE objective function reach a minimum at iteration F, the dissipated energy J and the power U continue to decrease as additional actuators are eliminated from the cantilever box beam. The Min $\Sigma\beta$ objective function remains unchanged from iteration F to iteration G. Therefore, iteration G is taken to be the optimum actuator configuration since it represents the least number of actuators which produces one of the best possible combinations of all of the original objective functions. Iteration G is equivalent to the optimal configuration in the aluminum case where the optimal configuration also comprised four actuators. From the study of optimal actuator thicknesses in the previous sections, it is known that the effective bending moment decreases for an increase in the value of Ψ which represents the ratio of box beam stiffness to actuator stiffness. Since the ratio Ψ is larger for steel than for aluminum, the same piezoelectric actuator produces a smaller effective bending moment using a steel box beam material. Therefore, the optimal piezoelectric thickness should increase for steel. The design variable iteration history is presented in table 4, where it is shown that actuator thicknesses are immediately driven to their upper bound from the initial design to the first iteration, as expected. Values of non-dimensional actuator thickness t^* are 0.18 and 0.20 for the optimal designs of

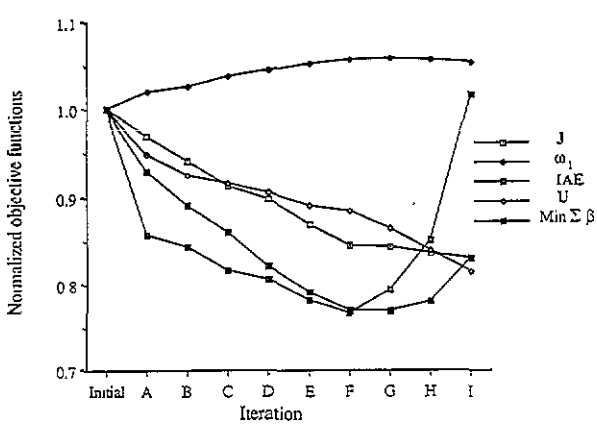

Figure 10. Normalized objective functions: steel.

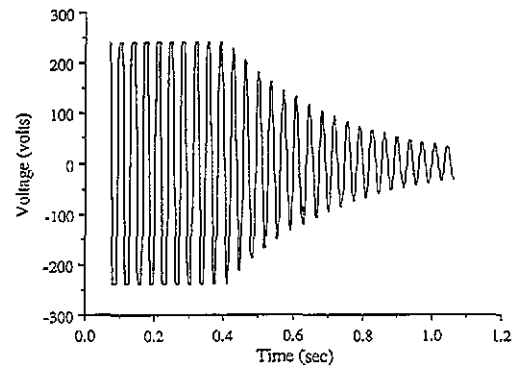

Figure 11. Voltage applied to actuator 1, iteration G: steel.

aluminum and steel box beam materials, respectively. Since these thicknesses represent the upper bound of currently available PZT sheets, it is clear that the optimal value of t^* for the static case is not practical for the cantilever box beam considered in this study. Usable actuator thicknesses are considerably less than the optimal values of t^* obtained in the static case. A higher gain is required at each iteration for the steel beam. The voltage constraint is active for a longer period of time than for aluminum in the optimal configuration, indicating reduced actuator effectiveness. The variation of voltage with time is presented in figure 11 for the actuator at element 1. Finally, figure 12 presents the variation of tip displacement with time, indicating that the displacement constraints are satisfied. The magnitude of tip displacement for the steel beam is 44% lower than that for the aluminum beam since steel is a stiffer material, although its mass is 22 kg compared to 10 kg for the aluminum beam.

7. Concluding remarks

A multiobjective optimization procedure is developed for the design of intelligent structures using piezoelectric materials for vibration control, which is based on the method of feasible directions. An approximation method is used to reduce the computational effort. A procedure is also developed to determine optimal actuator locations on a structure. Optimal piezoelectric actuator thicknesses are determined for the static case. The actuator location problem is then coupled with an optimization problem involving structure and control. Dissipated energy, electric power requirements, vibration and

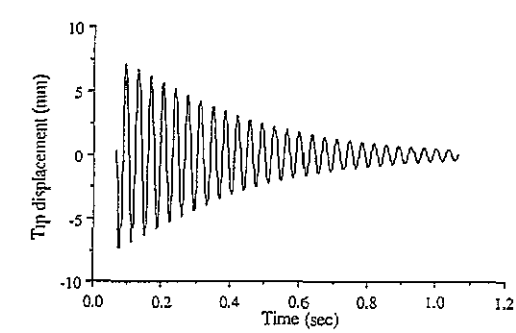

Figure 12. Tip displacement, iteration G: steel.

natural frequency are included as objective functions. Constraints are placed on vibration amplitudes, voltage applied to the actuators, mass and system energy. Design variables include cross sectional areas of structural members, actuator gains and actuator thicknesses. The optimization procedure is applied to a cantilever beam. Two different materials, aluminum and steel, are used. The following observations are made from this study.

(1) Stiffner piezoelectric materials were more desirable as actuators.

(2) Using PZT G-1195 piezoceramic actuators, the non-dimensional optimal actuator thickness, for the model developed in this research, in the static case was found to be significantly smaller (68%) for an aluminum box beam than for a steel box beam.

(3) Inclusion of dynamics effects had a significant impact on optimal actuator thickness. In case of a large number of actuators, optimal actuator thicknesses decreased due to the resulting weight penalty. In the case of a smaller number of actuators, the optimal thickness increased beyond currently available actuator thicknesses. Therefore, the thickest piezoceramic materials which can be obtained should be implemented in the optimum design.

(4) A reduced number of actuators was able to control the structure compared to the initial design, although the minimum number of actuators did not represent the optimum design.

Acknowledgments

The authors wish to acknowledge the support of their research through a grant from Arizona State University, Office of the Vice President of Research, Grant number XAR-E011.

References

Anderson E H, Moore D M and Fanson J L 1990 Development of an active truss element for control of precision structures *Opt. Eng.* **29** 1333–41

Bailey T and Hubbard J E Jr 1985 Distributed piezoelectric-polymer active vibration control of a cantilever beam *J. Guidance Control Dyn.* **8** 605–11

Bickford W B 1990 *A First Course in the Finite Element Method* (Boston, MA: Irwin)

Chaudhry Z and Rogers C A 1992 Enhanced structural control with discretely attached induced strain actuators *Proc. 33rd AIAA/ASME/ASCE/AHS/ASC Structures, Structural Dynamics and Materials Conf.* (Dallas, TX, 1992) pp 548, 554.

Chattopadhyay A and McCarthy T 1991 Multiobjective design optimization of helicopter rotor blades with multidisciplinary couplings *Structural Systems and Industrial Applications* ed S Hernandez and C A Brebbia pp 451–461

Chattopadhyay A and Seeley C E 1993 Application of design optimization techniques for vibration control of structures using piezoelectric devices *Proc. SPIE N. Am. Conf. on Smart Structures and Materials* (Albuquerque, NM, 1993)

Crawley E F and de Luis J 1987 Use of piezoelectric actuators as elements of intelligent structures *AIAA J.* **25** No 10 Oct. 1373–1385

Fadel G M, Riley M F and Barthelemy J F 1990 Two point exponential approximation method for structural optimization *Struct. Optimization* Vol 2, 117–124

Hanagud S, Obal M W and Meyyappa M 1985 Electronic damping techniques and active vibration control *Proc. 26th AIAA/ASME/ASCE/ASC Structures, Structural Dynamics and Materials Conf.* (Orlando, FL, 1985) pp 443–453

Hanagud S, Obal M W and Calise A J 1992 Optimal vibration control by the use of piezoceramic sensors and actuators *J. Guidance Contr. Dyn.* **15** 1199–1206

Heeg J 1991 An analytical and experimental study to investigate flutter suppression via piezoelectric actuation *Master's Thesis* George Washington University

Horner G and Walz J 1985 A design methodology for determining actuator gains in spacecraft vibration control *Proc. 26th AIAA/ASME/ASCE/ASC Structures, Structural Dynamics and Materials Conf.* (Orlando, FL, 1985) pp 143–151

Kim S J and Jones J D 1990 Optimal design of piezo-actuators for active noise and vibration control *AIAA 13th Aeroacoustics Conf.* (Tallahassee, FL, 1990) pp 1–11

Koht N S and Veley D E 1990 Robustness characteristics of optimum structural/control design *Proc. AIAA Guidance and Controls Meeting* (Portland, OR, 1990) pp 394–402

Koht N S, Venkayya V B, Eastep F E 1986 Optimal structural modifications to enhance the active vibration control of flexible structures *AIAA J.* **24** No 8 Aug 1368–1374

Kynar Piezo Film Technical Manual 1987 (Pennwalt Corporation)

Miller D F and Shim J 1987 Gradient-based combined structural and control optimization *J. Guidance Contr. Dyn.* **10** May–June 291–298

Ogata K 1990 *Modern Control Engineering* (Englewood Cliffs, NJ: Prentice-Hall)

Onoda J and Hanawa Y 1992 Optimal locations of actuators for statistical static shape control of large space structures: a comparison of approaches, *Proc. 33rd AIAA/ASME/ASCE/AHS/ASC Structures, Structural Dynamics and Materials Conf.* (Dallas, TX, 1992) pp 2788–2795

Rogers C A 1993 Smart structures: where does the energy go? *Invited Technical Talk, SPIE N. Am. Conf. on Smart Structures and Materials* (Albuquerque, NM, 1993)

Schulz G and Heimbold G 1983 Dislocated actuator/sensor positioning and feedback design for flexible structures *J. Guidance* Vol 6 No 5 Sept.–Oct. 1983 361–367

Sepulveda A E, Jin I M and Schmit L A Jr 1992 Optimal placement of active elements in control augmented structural synthesis *Proc. 33rd AIAA/ASME/ASCE/AHS/ASC Structures, Structural Dynamics and Materials Conf.* (Dallas, TX 1992) pp 2768–2781

Vanderplaats G N 1973 *CONMIN—A FORTRAN Program for Constrained Function Minimization* User's Manual. NASA TMX-62 282